Characterization of instrumental background in (p,γ) reaction studies

T Bokhutlo[1,2], R Neveling[2], CO Kureba[1], KL Malatji[2,4], LM Donaldson[2], P Adsley[7], A Bahini[2], JAC Bekker[2,5,], SD Binda[2,5], L Jafta[2,9], P Jones[2], S Jongile[2], TC Khumalo[2], SPE Magagula[2,5], TG Modise[2,10] RE Molaeng[2,5], AA Netshiya[2,5,6], L Pellegri[2,5] and M Wiedeking[2,3,5]

[1]Department of Physics and Astronomy, Botswana International University of Science and Technology, Palapye, Botswana
[2]iThemba LABS, Cape town, South Africa
[3]Lawrence Berkeley National Laboratory, Berkeley, California, USA
[4] Department of Nuclear Engineering, University of California, Berkeley, USA
[5]School of Physics, University of the Witwatersrand, Johannesburg, South Africa
[6]Department of chemical and physical science, Walter Sisulu University, Mthatha, South Africa.
[7]Cyclotron Institute, Texas A&M University, College Station, Texas, USA
[8]Department of Physics, University of Cape Town, Cape Town, South Africa
[9]Department of Physics and Astronomy, University of the Western Cape, Cape town, South Africa
[10] Department of Physics, University of Botswana, Gaborone, Botswana

E-mail: bt23019064@biust.ac.bw

Abstract. Understanding and mitigating background radiation is essential for high-precision experiments. This work investigates background contributions in radiative proton-capture measurements at the low-energy nuclear astrophysics beamline of the iThemba LABS Tandetron facility. These experiments aim to study the statistical properties of proton-rich nuclei, particularly the Photon Strength Function (PSF), via charged particle capture reactions. However, accurate extraction of physical observables can be challenging due to the presence of instrumental background arising from beam interactions with materials other than the target. This study presents a systematic characterization of such background, identifying key sources and evaluating their impact on the measured spectra.

1 Introduction

Radiative capture reactions are essential for probing how excited nuclei undergo electromagnetic decay. Of particular interest is the Photon Strength Function (PSF), which characterizes the average reduced transition probability for gamma-ray emission or absorption within a nucleus [1]. PSFs play a vital role in modeling nuclear reaction rates in astrophysical environments and nuclear reactors. In a typical radiative capture reaction, such as the (p,γ) reaction, the proton is captured by a nucleus to form an excited compound system that de-excites via gamma emission [1]. The energies and intensities of these emitted gamma rays provide insights into the nuclear level structure and electromagnetic transition probabilities associated with the compound nucleus. In precision nuclear measurements, isolating events produced by the reaction of interest from background-induced artifacts can be crucial to ensure accurate results. This study reports on results obtained at the H-line of the iThemba LABS 3 MV Tandetron facility, where a proton beam was used for PSF investigations. Initial experiments revealed anomalous structures that did not originate from the target material. This work aims to identify potential sources of background, a necessary prerequisite for implementing appropriate mitigation measures.

2 Experimental Setup

The 3 MV Tandetron accelerator was installed in 2017 at iThemba LABS after the 6 MV Van de Graaff accelerator was decommissioned. The accelerator is capable of producing a terminal voltage of up to 3 MV, delivering particle beams with intensities of up to 150 μA [2]. The facility supports rapid switching between light and heavy ion beams of protons, alphas and ^{3}He, providing enhanced flexibility for multidisciplinary research. Currently the following beam lines are connected to the accelerator: low energy nuclear astrophysics array (H-line), particle induced x-ray emission array (K-line), and Rutherford Backscattering spectrometry (M-line) [2].

The H-line, which is illustrated in fig. 1 is used to study radiative capture reactions. Relevant beamline elements directly upstream from the scattering chamber include three quadrupole magnets and a set of vertical and horizontal steerer magnets. In addition, a removable Faraday cup and a beam profiler positioned in front of the cup are used to measure the beam's intensity and shape before it enters the quadrupole triplet section. The aluminum scattering chamber has a spherical shape with a 12 cm diameter to allow for a small distance between the target and the gamma detectors placed around the scattering chamber. Inside the scattering chamber is an aluminum target ladder with 4 holders, which can be changed manually without breaking vacuum. At approximately 850 mm downstream from the scattering chamber is a fixed faraday cup shielding which is 5 cm thick. This Faraday cup consists of a 55.5 mm diameter high-conductivity copper cup. The assembly includes multiple copper components (e.g. core block, outer casing, inlet and outlet pipes) and is supported by Shapal-M ceramic insulating bushings for electrical isolation. Magnetic suppression is achieved via permanent $SmCo_5$ magnets (Vacomax 145) mounted with magnet steel, which helps to deflect secondary electrons. The entire unit is soldered under vacuum conditions, ensuring high vacuum integrity. The cup is mounted using a stainless steel (304) frame and fasteners to provide mechanical stability within the beamline environment.

The detector support structure surrounding the scattering chamber consists of an angular distribution table on the beam right side, and a subset of the original AFRODITE [3] detector frame on the beam left side. For the first few experiments on the H-line, the high purity Germanium (HPGe) Clover detectors [4] as well as large volume 3.5"x8" $LaBr_3$:Ce detectors [5] available at iThemba LABS were used to populate the detector support structure. The angular distribution table can accommodate 3 HPGe Clover detectors over a wide range of angles (26° - 141°). The old AFRODITE frame has 15 available positions, of which 4 are meant for small detectors such as the 2"x2" $LaBr_3$:Ce detectors. Of the remaining 11 positions, space limitations imposed by the beamline infrastructure result in only 8 being accessible for the available HPGe Clover detectors. Alternatively, 9 positions are accessible for large volume 3.5"x8" $LaBr_3$:Ce detectors. These positions are at the polar angles (i.e. relative to the beam direction which defines the polar axis) of 45°, 90° and 135°.

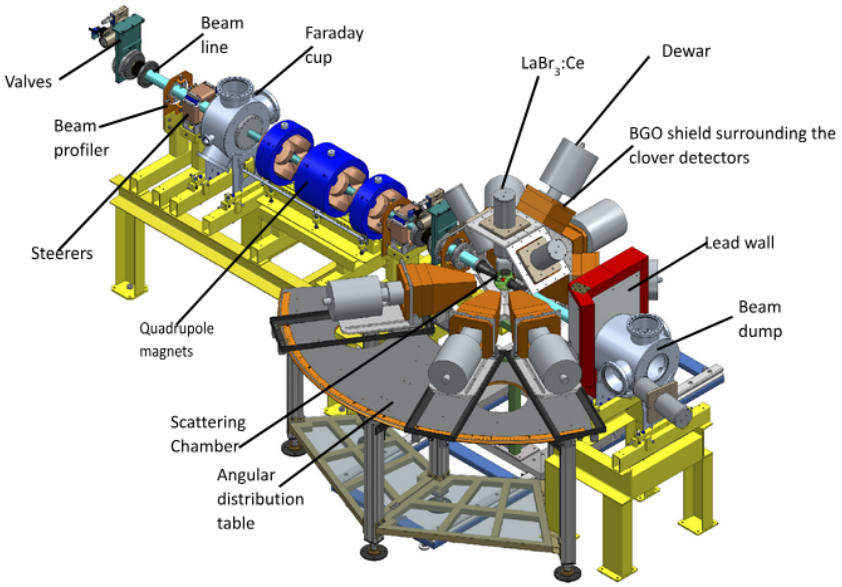

Figure 1: A schematic overview of the H-line at the iThemba LABS Tandetron facility.

3 Results and Analysis

This is a newly established facility and, so far only three datasets have been acquired. In this work, the focus is placed on the first experiment performed in 2023, which investigated the ^{60}Ni(p,γ)^{61}Cu reaction over a proton energy range of 2.24 to 4.32 MeV, with measurements taken at 31 beam energies spaced at intervals of 60–80 keV apart [6]. The ^{60}Ni target had an areal density of 1 mg/cm^2. The experimental setup employed a total of four HPGe detectors and three $LaBr_3$:Ce detectors for gamma-ray detection. Among the four HPGe detectors, two

were mounted on the Half-AFRODITE frame, one at at 90° and one at at 135°, while the remaining two were positioned on the table: one at 90° and the other at 135°. The three Labr:Ce_3 detectors were also mounted on the half-AFRODITE frame, with two placed at 90° and the third positioned at 45°. By combining high resolution HPGe detectors and fast response $LaBr_3$:Ce detectors, the setup allowed for both precise energy determination and time coincidence measurements, enhancing the overall efficiency and time resolution of the experiment.

The Q-value of the ^{60}Ni(p,γ)^{61}Cu reaction is 4799.8 keV; consequently, for a beam energy of e.g.E_p = 2480 keV, the direct gamma transition to the ground state from the highest excited populated energy level is expected to at 7279.8 keV, excluding energy loss through the target and recoil energy of the residual nuclei. The expectation is that this should be the highest prompt gamma-ray energy observed in the detectors and Compton background, considering the ideal conditions where the beam only interacts with the nuclei in the target foil. Furthermore, since the proton beam will lose some energy ΔE_{tgt} as it passes through the target, one can expect a group of high energy gamma-rays to appear from from (E_p+Q) to (E_p+Q-ΔE_{tgt}), depending on the availability of states in ^{61}Cu to be populated. Other than the first and second escape peaks in the HPGe detectors, one also expects to see peaks in the gamma-energy spectrum represented by the decay from the highly excited ^{61}Cu nucleus decaying to its low-lying excited states, such as any of the following: 475 keV 1/2$^-$, 870 keV 5/2$^-$, 1310 keV 7/2$^-$, 1394 keV 5/2$^-$ etc. However, what is observed as shown in Fig. 2), are strong and very broad structures between 5 and 7 MeV (especially at the lower beam energies) as well as clear peak structures at energies higher than expected from the ^{60}Ni(p,γ)^{61}Cu reaction.

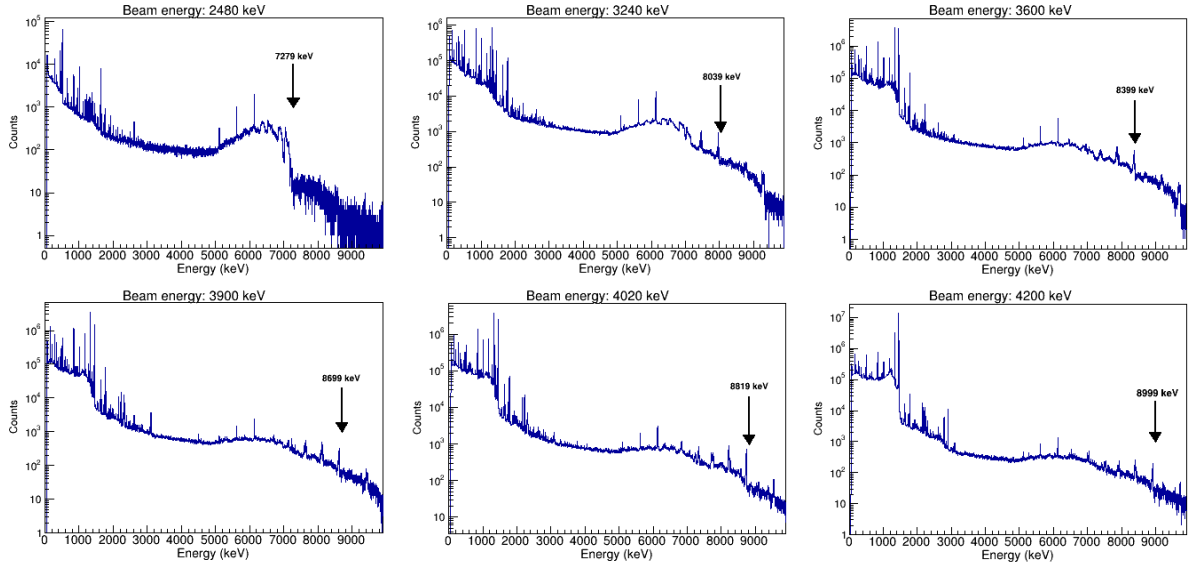

Figure 2: Gamma-ray energy spectra obtained with a single HPGe detector placed at 135° degrees for the ^{60}Ni(p,γ) radiative capture reaction for different beam energies. The arrows indicate the position of the highest expected gamma-ray transitions from ^{61}Cu compound nuclei.

The impact of environmental background can be assessed through data acquired ideally without beam. Unfortunately, the only data available are for an empty target run, i.e. without a target but with beam only. Well-known low-energy gamma rays such as those appearing at 1460 keV (^{40}K) and at 2614 keV (^{232}Th decay chain) are shown in Fig. 3(a). Since there were three $LaBr_3$:Ce detectors placed close to the HPGe detectors, intrinsic $LaBr_3$:Ce activity can be observed at 788 keV and 1436 keV. Contributions from these sources to the observed spectra were minimal during the experiment. Next, one can ascertain whether the background comes from a badly tuned beam interacting with beamline elements upstream of the target, as well as the target frame itself, by looking at data from the empty target beam run. Ion-optical calculations show [7] that a properly tuned beam has a sufficiently small cross section and remains well within the 60.5 mm diameter of the beam pipe, posing no risk of contact with the walls. Observations using a scintillating beam viewer at the target position confirm that the beam can achieve a diameter of less than 2 mm at the target location. Given that the target frame has an opening of 8 mm (height) by 14 mm (width), a well-tuned beam should easily pass through without striking the frame. Furthermore, ion-optical calculations indicate that the nominal beam diameter at the beam stop is approximately 7 mm. For a well-tuned beam, the most likely cause of background from upstream of the target must be from slit scattering at the beamline slits closer to the Tandetron, or the curved beampipe from the switching magnet.

The empty target spectrum shown in Fig .3(b) reveals a similar structure between 5 and 7 MeV as seen with beam (see Fig. 2 top left), but much reduced in intensity. While it is not impossible for stray beam particles to interact with beamline elements to cause some background, clearly the bulk of the background did not originate from

sources upstream of the target, or by beam "halo" created upstream from the target to interact with beamline elements at the target and downstream of the target. Since the majority of the background only becomes apparent when the beam interacts with the ^{60}Ni target, one has to consider either some level of target contamination, or that the interaction with the target influences the beam to interact with the beampipe or other hardware downstream from the target.

Indeed, in the presence of the target, the observed gamma-ray spectra contain a number of background peaks. These peaks were consistently observed for all beam energies. Gamma rays at low energies are observed for the nuclei ^{27}Al, ^{28}Si, ^{56}Fe, ^{57}Co, ^{60}Ni and ^{61}Cu, which result from (p,p') and (p,γ) reactions from ^{27}Al, ^{56}Fe and ^{60}Ni. This is shown in Fig. 3(c). While one would expect the gammas from interaction with ^{60}Ni, the contributions from ^{27}Al and ^{56}Fe are concerning, since it implies that a significant number of protons interact with nuclei that are not in the target foil. The question is thus: how do the protons, supposedly well focused onto the target, end up hitting signicant amounts of ^{27}Al and ^{56}Fe? In addition, the structures between 5 and 7 MeV are known to originate from the ^{19}F(p,$\alpha\gamma$)^{16}O reaction [8]. The gamma rays at 6.128(4), 6.917(6), and 7.116(14) MeV from ^{16}O decay are highlighted in Fig. 3(d). The states at 6.9171(6) and 7.11685(14) MeV exhibit pronounced Doppler broadening as a consequence of their very short (few femtosecond) half-life. These broad structures makes it more difficult to identify and resolve the gamma rays originating from the particle capture reactions, and complicates spectral analysis. Finally, the fact that there are high-energy gamma rays beyond those expected from the ^{60}Ni(p,γ) reaction implies that proton capture reactions on nuclei with higher Q-values are also being observed. The arrow in Fig. 3(e) indicates a structure of observed high-energy gamma rays consistent with the ^{56}Fe(p,γ)^{57}Co reaction, which has a Q-value of 6027 keV.

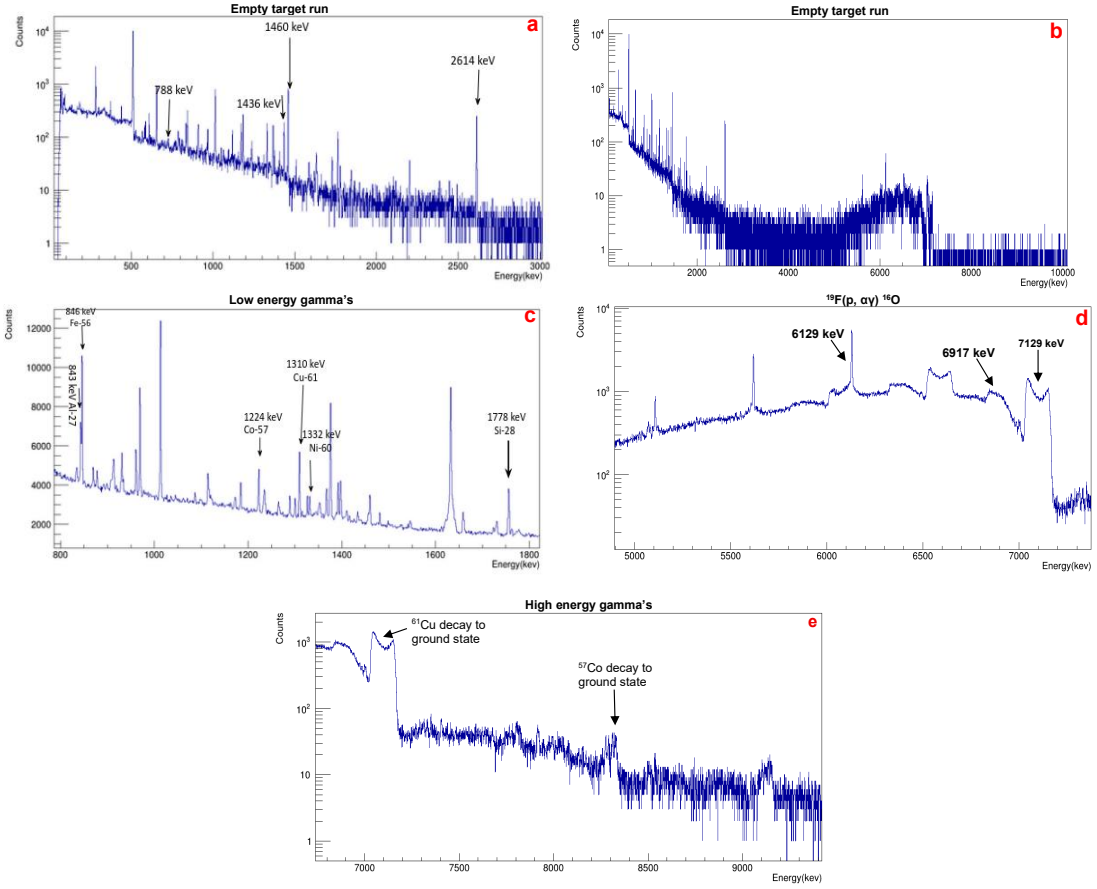

Figure 3: Identification of different backgrounds from ^{60}Ni(p,γ) at E_{beam}= 2.24 MeV: a) environmental background and radiation from the $LaBr_3$:Ce detector, b) empty target run showing the full gamma-ray energy range, c) low-energy gamma rays from a target-in run, d) oxygen related structures originating from the ^{19}F(p,$\alpha\gamma$) reaction and e) high-energy gamma rays corresponding to direct transitions to the ground state.

4 Background Characterization

It is evident that the majority of the background arises from proton interactions with ^{19}F, ^{27}Al, and ^{56}Fe. A key piece of evidence in identifying the location of these interactions is the beam intensity measured at the fixed Fara-

day cup located at the end of the beamline. When an empty target frame is used, the beam current measured by the removable Faraday cup upstream of the target agrees with the reading on the fixed Faraday cup, indicating minimal loss. In contrast, when a ^{60}Ni target is inserted, the fixed Faraday cup registers only about 60% of the beam current delivered. It is, therefore, clear that introduction of the target causes both beam intensity loss as well as a dramatic background increase. To investigate how the introduction of the 1 mg/cm^2 thick ^{60}Ni target can lead to beam intensity loss on the Faraday cup, an SRIM simulation was performed where 10,000 protons at an energy of 4.020 MeV were directed perpendicular onto a 1 mg/cm^2 thick ^{60}Ni foil. The results of the simulation revealed that a significant percentage of these protons undergo angular deviation from their original trajectory after traversing the target. These redirected protons intersect with parts of the the scattering chamber and the beampipe, as shown in Fig. 4.

The scattering chamber is mostly made of aluminum (which only has one stable isotope, namely ^{27}Al), but also has some Vesconite components. The conical section between the scattering chamber and the beam line connecting the chamber is made of Vesconite, while the main beampipe downstream of the scattering chamber all the way to the beam stop is made of stainless steel. Vesconite is a self-lubricating polymer commonly used in vacuum and beamline assemblies due to its mechanical strength, thermal stability, and low out-gassing properties. However, as highlighted [8], Vesconite contains a significant amount of fluorine, originating from its polytetrafluoroethylene (PTFE) based composition. In [8] they studied beamline-induced backgrounds observing the intense gamma-ray emission resulting from proton interactions with Vesconite, specifically from the ^{19}F(p,$\alpha\gamma$)^{16}O reaction, which produces high-energy gamma lines at at 6.128(4), 6.917(6), and 7.116(14) MeV. Stainless steel, which contains iron, nickel, and chromium, is known to contribute to gamma-ray background through reactions like ^{56}Fe(p,γ)^{57}Co and ^{60}Ni(p,γ)^{61}Cu.

A distinction is made below between three distinct downstream beamline components. Firstly, protons deflected at large angles between 90° and 63.4° strike the interior walls of the scattering chamber. As it is made of both aluminum and Vesconite, it is a potential source of background gamma rays through reactions such as ^{27}Al(p,γ)^{28}Si and ^{19}F(p,$\alpha\gamma$)^{16}O. Although these high-angle deviations represent a small fraction of the beam (estimated at less than 5%), they are important due to the amount of material with which the protons can interact. Secondly, a substantial fraction of the beam, estimated around 6%, was found to exit the target at intermediate angles between 26.6° and 63.4°, leading to interact with the Vesconite cone located between the scattering chamber and the main beamline, and thus contributes to fluorine-induced background features. Lastly, proton deviation between 3.03° and 26.6°, representing the most dominant post-target trajectories at an estimated 20% of the incident protons, will hit the inner walls of the stainless steel beam pipe.

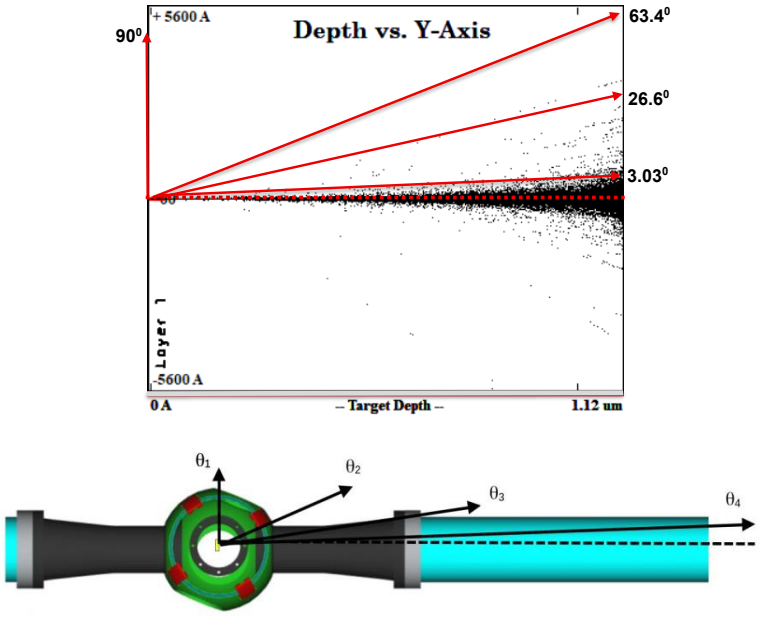

Figure 4: SRIM simulation showing the angular distribution of protons transmitted through a 1 mg/cm^2 ^{60}Ni target. The plot highlights four distinct angular paths corresponding to interactions with different downstream components. These angles represent beam divergence due to multiple scattering and indicate where post-target interactions are likely to occur, contributing to instrumental background.

5 Summary and Conclusion

This study investigated the sources of instrumental background in radiative proton capture (p,γ) experiments at the iThemba LABS Tandetron facility, with a focus on improving the extraction of gamma-ray strength functions (PSFs). Through gamma-ray spectroscopy, SRIM simulations, and beam diagnostics, it was shown that post-target beam divergence leads to unintended interactions with surrounding beamline components, including the scattering chamber, the Vesconite beamline tube, and the stainless steel beam pipe. These interactions give rise to background gamma rays, particularly from reactions on ^{27}Al, ^{56}Fe, and ^{19}F. A major contributor to high-energy background was the ^{19}F(p,$\alpha\ \gamma$)^{16}O reaction, producing Doppler-broadened gamma rays from PTFE-based Vesconite components. To mitigate these effects, several recommendations are proposed.

Firstly, to reduce the impact of the strong oxygen peaks from the ^{19}F(p,$\alpha\gamma$) reaction, efforts should focus on minimizing the amount of Vesconite in the setup. A key step is replacing the conical beamline components made of Vesconite with aluminum. Although this substitution may increase aluminum-induced background, such background is relatively minor in the 5–7 MeV energy range, which is currently dominated by gamma-ray background from oxygen. Secondly, the possibility to have a high-Z collimator downstream from the target should be investigated. The high proton number will imply a high Coulomb barrier, which means that the material is not likely to undergo nuclear reactions and contribute to the gamma ray spectrum. Such a collimator should be connected to the beam current measurement, and should be positioned close enough to the target so that it can intercept most of the angular beam spread before the beam can interact with any of the beamline elements. Implementing these improvements is expected to significantly enhance the signal-to-noise ratio, enabling more accurate and reliable measurement of weak gamma transitions. The findings serve as an essential step toward establishing a low-background, high-precision experimental platform for nuclear astrophysics research at iThemba LABS Tandetron facility.

6 Acknowledgments

The authors would like to thank the accelerator team at the Tandetron facility of iThemba LABS for providing high quality experimental conditions, as well as the Research and Development Technical Support (RDTS) team for their assistance with the design, software, and detector maintenance. This research was supported in part by the National Research Foundation (NRF) of South Africa (Grant No's. 118846, 92600, 90741, 92789, and REP_SARC180529336567). Additional support was provided by the U.S. Department of Energy, Office of Science, Office of Nuclear Physics under Contract No. DE-AC02-05CH11231 The financial assistance of the NRF and iThemba LABS is gratefully acknowledged. Any opinions, findings, and conclusions expressed in this material are those of the authors and do not necessarily reflect the views of the NRF.

References

[1] S. Goriely, A. Bauswein, and H.-T. Janka, "R-process nucleosynthesis in dynamically ejected matter of neutron star mergers," *The European Physical Journal A*, vol. 55, no. 10, p. 172, 2019. [Online]. Available: https://doi.org/10.1140/epja/i2019-12801-2

[2] Z. Khumalo, C. Mtshali, M. Msimanga, N. Mongwaketsi, and F. Mashele, "A new 3 MV Tandetron™ accelerator at iThemba Laboratory for Accelerator-Based Sciences," *Journal of Instrumentation*, vol. 20, no. 06, p. T06001, jun 2025. [Online]. Available: https://dx.doi.org/10.1088/1748-0221/20/06/T06001

[3] M. Lipoglavšek, N. Soić, A. Palacz, T. O. Tuček, S. Širca, P. Vidmar, M. Korolija, M. Lozar, J. Mrazek, N. H. Medina, D. G. Jenkins, R. L. Gill, and D. S. Haslip, "High-resolution γ-ray spectroscopy with an array of clover detectors at the beam line of a tandem accelerator," *Nuclear Instruments and Methods in Physics Research Section A: Accelerators, Spectrometers, Detectors and Associated Equipment*, vol. 557, pp. 523–527, 2006.

[4] G. Duchêne, F. Beck, P. Twin, G. de France, D. Curien, L. Han, C. Beausang, M. Bentley, P. Nolan, and J. Simpson, "The clover: A new generation of composite Ge detectors," *Nuclear Instruments and Methods in Physics Research Section A: Accelerators, Spectrometers, Detectors and Associated Equipment*, vol. 432, pp. 90–110, 1999.

[5] E. V. D. V. Loef, P. Dorenbos, C. W. E. V. Eijk, K. Krämer, and H. U. Güdel, "High-energy-resolution scintillator: Ce^{3+} activated $LaBr_3$:Ce," *Applied Physics Letters*, vol. 79, no. 10, pp. 1573–1575, 2001.

[6] M. Wiedeking, "Testing the validity of the Brink-Axel hypothesis," Feb. 2020, iThemba LABS research proposal.

[7] H. Barnard, Private communication, 2024, iThemba LABS.

[8] D. Dell'Aquila and M. Vigilante, "An overview of the $^{19}\mathrm{F}(p,\alpha_0)^{16}\mathrm{O}$ reaction with direct methods," in *Journal of Physics: Conference Series*, vol. 703, no. 1, 2016, p. 012015. [Online]. Available: https://doi.org/10.1088/1742-6596/703/1/012015